

ARTICLE OPEN



JMJD1C promotes smooth muscle cell proliferation by activating glycolysis in pulmonary arterial hypertension

Chen Zhang¹, Yue Sun², Yingying Guo², Jingjing Xu² and Haiyan Zhao²✉

© The Author(s) 2023

Pulmonary arterial hypertension (PAH) is a chronic disorder characterized by hyperproliferation of pulmonary arterial smooth muscle cells (PASMCs). JMJD1C, a member of the Jumonji domain containing C (JMJC) histone demethylase family, contributes to cardiovascular dysfunction. However, the role of JMJD1C in PAH remains unknown. Mice were exposed to hypoxia to mimic several features associated with PAH clinically. We found that JMJD1C was highly expressed in the lungs of mice after hypoxia exposure. JMJD1C knockdown ameliorated hypoxia-induced right ventricular remodeling and thickening of the pulmonary arterial wall. PASMC hyperproliferation and resistance to apoptosis in mice exposed to hypoxia were suppressed by JMJD1C inhibition. We demonstrated that JMJD1C silencing reduced glycolytic enzymes (HK2, PGK1 and LDHA) and lactate overaccumulation in the lungs of mice exposed to hypoxia. In vitro, hypoxia-induced hyperproliferation and activated glycolytic processes in mouse PASMCs were impaired by JMJD1C knockdown. In addition, the activation of STAT3 signaling by hypoxia was suppressed by JMJD1C silencing both in vivo and in vitro. The overexpression of STAT3 reversed the inhibitory effect of JMJD1C depletion on proliferation and glycolysis in PASMCs under hypoxia. Thus, JMJD1C induces glycolytic processes by activating STAT3 signaling to promote PASMC proliferation and pulmonary vascular remodeling, suggesting the potential role of JMJD1C in regulating the metabolic program and vascular remodeling in PAH.

Cell Death Discovery (2023)9:98; <https://doi.org/10.1038/s41420-023-01390-5>

INTRODUCTION

Pulmonary arterial hypertension (PAH) is a rare and fatal cardiopulmonary disease characterized by a progressive increase in pulmonary vascular resistance and pulmonary vessel remodeling, which ultimately leads to right ventricular failure and death [1]. Vasoconstriction, endothelial cell dysfunction, smooth muscle cell proliferation, extracellular matrix accumulation, and inflammation are important processes associated with PAH [2]. Although current therapies can improve symptoms and hemodynamic parameters in PAH, they do not significantly reduce morbidity and mortality. Thus, novel approaches for treating PAH are urgently needed.

Glycolysis, or the Warburg effect, has been suggested to be a critical pathogenic pathway in the development of PAH [3]. Positron emission tomography shows dramatic glucose uptake in the lungs of idiopathic PAH patients, indicating increased glycolytic activity in the lungs during PAH [4]. In addition, it has been demonstrated that both pulmonary arterial smooth muscle cells (PASMCs) and endothelial cells from patients or animals with PAH undergo significant glycolysis and then hyperproliferate [5]. PASMCs are one of the major cell types that affect vascular remodeling in PAH, and these cells exhibit several pathological features, such as hyperproliferation, resistance to apoptosis and metabolic disturbances [6]. Kovacs et al. suggested that aberrant glycolysis contributed to significant collagen synthesis and

proliferation in PASMCs during PAH with vascular remodeling [7]. The underlying mechanisms of glycolysis in PASMCs still need further investigation.

JMJD1C is a member of the Jumonji domain containing C (JMJC) family, and it functions as a histone demethylase to activate gene transcription [8, 9]. For example, Viscarra et al. showed that JMJD1C regulated the lipogenic process by demethylating H3K9 at lipogenic promoters [10]. Chen et al. found that JMJD1C acted as a critical transcriptional coactivator to regulate the survival of acute myeloid leukemia cells [11]. Furthermore, a previous study by Lynch et al. indicated that JMJD1C had an effect on glycolytic and oxidative programs in HOXA9-dependent leukemogenesis [12]. Zhang et al. demonstrated that JMJD1C accelerated angiotensin II-induced cardiac hypertrophy and fibrosis in experimental mouse models [13, 14]. More importantly, microarray analysis showed significantly high expression of JMJD1C in the lungs of PAH patients, suggesting an association between JMJD1C and the risk of PAH [15]. However, the effect of JMJD1C on the development of PAH remains unknown.

In this study, mice or PASMCs were exposed to hypoxia to investigate whether JMJD1C knockdown affected the development of PAH. The glycolytic process was mediated by the STAT3 signaling pathway and was investigated to uncover the underlying mechanism of JMJD1C.

¹Department of Obstetrics and Gynecology, Shengjing Hospital of China Medical University, Shenyang, China. ²Department of Rheumatology and Immunology, Shengjing Hospital of China Medical University, Shenyang, China. ✉email: zhaohy5@sj-hospital.org

Received: 23 June 2022 Revised: 23 February 2023 Accepted: 28 February 2023

Published online: 18 March 2023

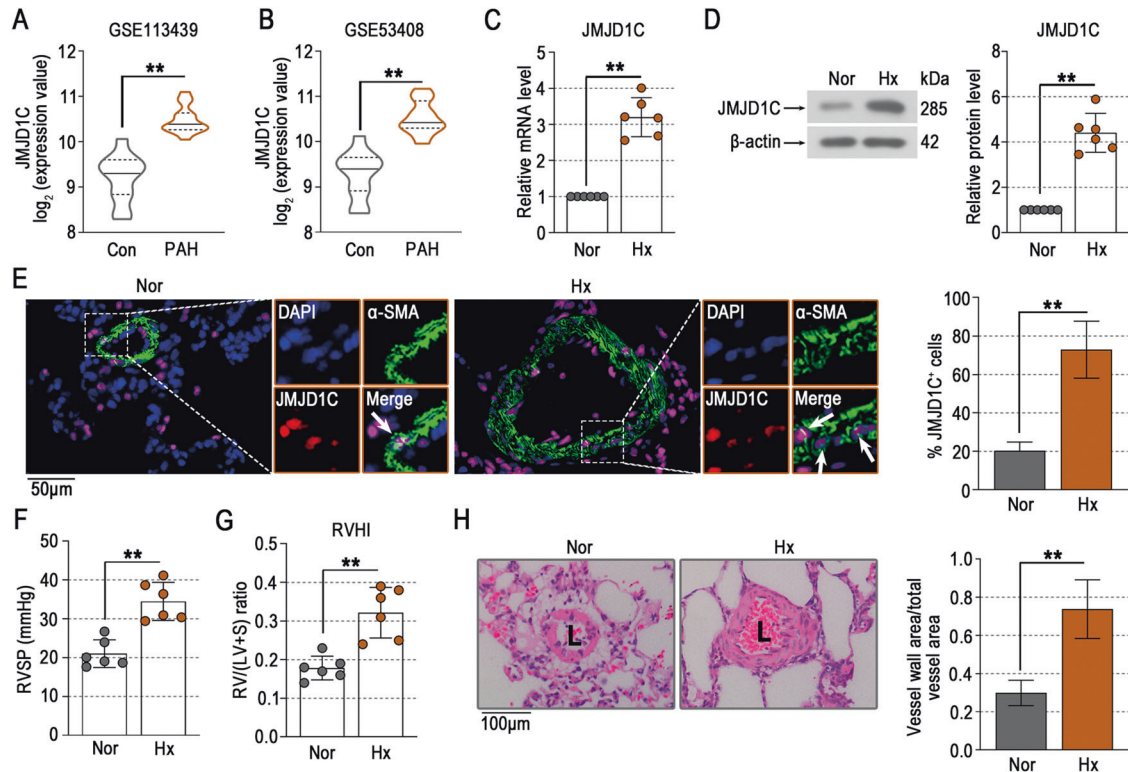


Fig. 1 JMJD1C expression is increased in the lungs of mice exposed to hypoxia. **A, B** Expression levels of JMJD1C mRNA in lung homogenates of PAH patients in GSE113439 and GSE53408. $N = 11-15$. **C, D** Relative mRNA and protein levels of JMJD1C in the lung were examined by qPCR and Western blotting. **E** Representative lung tissue sections were subjected to immunofluorescence staining of α -SMA (green) and JMJD1C (red). DAPI was used to stain cell nuclei (blue). Bar = 50 μ m. Arrows indicate the coexpression of α -SMA and JMJD1C in pulmonary arteries. **F, G** The RVSP, and RVHI were determined in mice exposed to normoxia or hypoxia. **H** Representative histological images of lung sections stained with hematoxylin and eosin (H&E). The wall thickness of the pulmonary arteries was measured. Bar = 100 μ m. Nor normoxia; Hx hypoxia; L Lumen. The values are the mean \pm SD, and statistical significance was assessed by unpaired t-test. $N = 6$, $***p < 0.01$.

RESULTS

JMJD1C expression is increased in the lungs of mice exposed to hypoxia

The dysregulated genes in the lung homogenates of PAH patients were downregulated, as shown by the Gene Expression Omnibus (GEO) [16] under accession numbers GSE113439 and GSE53408. The microarray data from GSE113439 and GSE53408 showed that the mRNA level of JMJD1C was increased in PAH patients (Fig. 1A, B). Similar alterations in JMJD1C at both the mRNA and protein levels were observed in the lungs of mice exposed to hypoxia (Fig. 1C, D). The immunofluorescence staining results suggested a high expression level of JMJD1C in the smooth muscle cells of mice exposed to hypoxia (Fig. 1E). Right ventricular remodeling was observed in mice exposed to hypoxia, as evidenced by increases in the right ventricular systolic pressure (RVSP) and right ventricular hypertrophy index (RVHI) (Fig. 1F, G). The thickness of the pulmonary arterial wall was also increased by hypoxia, as shown by HE staining (Fig. 1H). This finding suggests that high expression of JMJD1C may participate in the development of pulmonary hypertension.

JMJD1C knockdown attenuates pathological changes in mice exposed to hypoxia

AAV2 vectors for JMJD1C knockdown were used to study its role in pulmonary hypertension, and the protocol timeline is shown in Fig. 2A. We demonstrated that JMJD1C knockdown inhibited hypoxia-induced increases in RVSP and RVHI (Fig. 2B, C). Right ventricular hypertrophy and pulmonary arterial wall thickening in mice exposed to hypoxia were attenuated by JMJD1C inhibition (Fig. 2D, E). Taken together, these results suggest that JMJD1C contributes to the development of right ventricular hypertrophy

and pulmonary arterial remodeling in response to hypoxia exposure.

JMJD1C knockdown decreases PASM hyperproliferation and resistance to apoptosis in mice exposed to hypoxia

For the JMJD1C knockdown studies, we found that the mRNA and protein levels of JMJD1C in the lungs of mice exposed to hypoxia were reduced by AAV administration (Fig. 3A, B). The results of JMJD1C⁺ α -SMA⁺ immunofluorescence staining showed that JMJD1C knockdown inhibited hypoxia-induced JMJD1C enhancement in the PSMCs of mice (Fig. 3C). This finding indicates the potential role of JMJD1C in the changes in PSMCs during PAH.

PASM hyperproliferation and resistance to apoptosis are key events during PAH development. The results of Ki67 staining showed that hypoxia-induced PASM hyperproliferation was inhibited by JMJD1C depletion in vivo (Fig. 3D). The hypoxia-induced reduction in TUNEL-positive PSMCs was increased by JMJD1C knockdown (Fig. 3E). Taken together, these data suggest that JMJD1C promotes PASM hyperproliferation and resistance to apoptosis in mice exposed to hypoxia.

JMJD1C knockdown prevents glycolysis in mice exposed to hypoxia

Glycolysis is an important step in the production of ATP and lactate, and it drives the hyperproliferation of PSMCs during pulmonary hypertension development. We examined the expression of glycolytic enzymes, including hexokinase II (HK2), phosphoglycerate kinase 1 (PGK1) and lactate dehydrogenase A (LDHA), to evaluate the effect of JMJD1C on PAH. The results showed that the hypoxia-induced increase in glycolytic enzymes at the mRNA and protein levels in lung homogenates was reduced

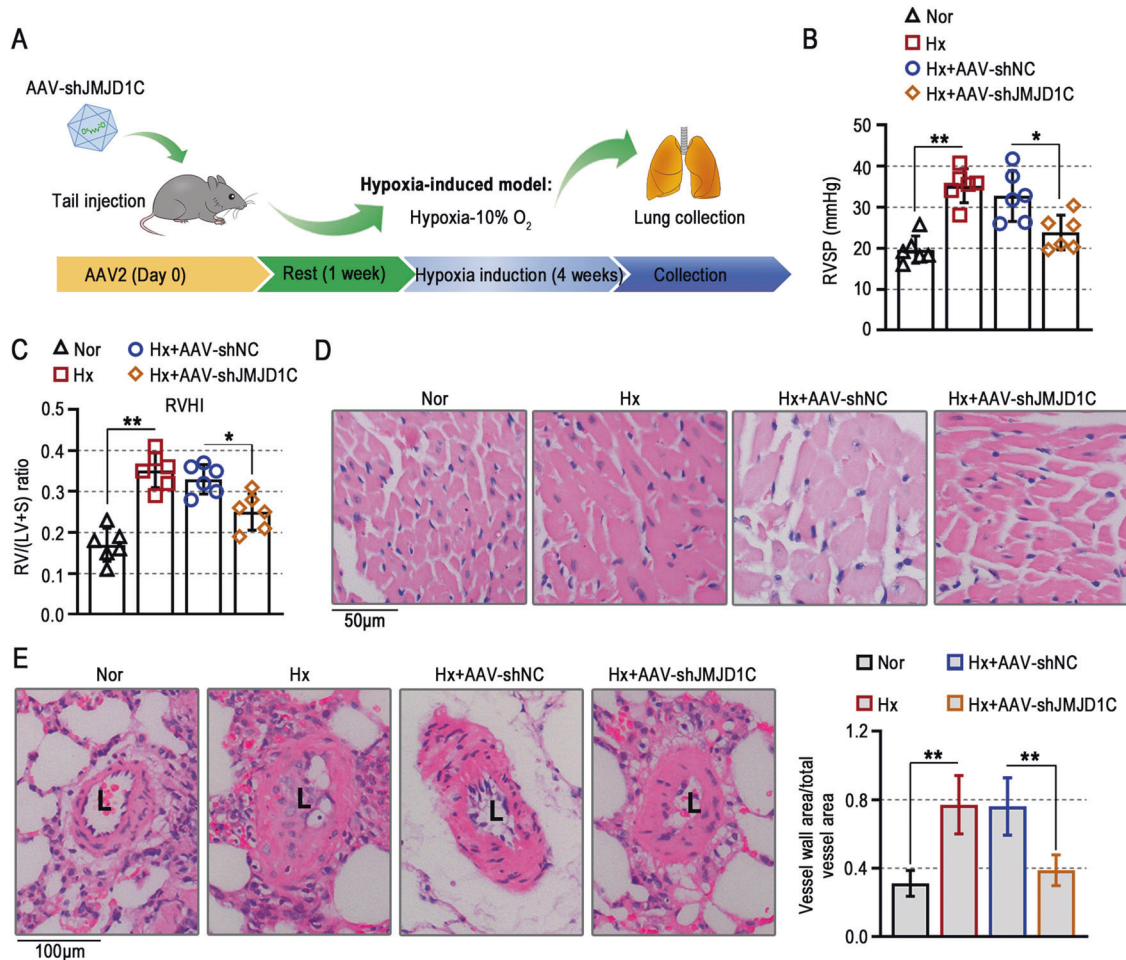


Fig. 2 JMJD1C knockdown attenuates pathological changes in mice exposed to hypoxia. **A** Illustration of the animal protocols. **B, C** The RVSP and RVHI in mice exposed to normoxia or hypoxia were examined. **D** Representative histological images of heart sections stained with H&E. Bar = 50 μ m. **E** Representative histological images of lung sections stained with H&E. The wall thickness of the pulmonary arteries was measured. Bar = 100 μ m. Nor Normoxia, Hx Hypoxia, L Lumen. The values are the mean \pm SD, and statistical significance was determined by one-way ANOVA. $N = 6$, * $p < 0.05$, ** $p < 0.01$.

by JMJD1C knockdown (Fig. 4A, B). Lactate is an end product of glycolysis, and we demonstrated that JMJD1C silencing inhibited hypoxia-induced lactate overaccumulation in the serum of mice (Fig. 4C). In addition, the increase in the phosphorylation of STAT3 in the lungs of mice exposed to hypoxia was prevented by JMJD1C knockdown (Fig. 4D). These results suggest that JMJD1C enhances glycolysis in hypoxia-induced pulmonary hypertension.

JMJD1C expression is upregulated in PSMCs exposed to hypoxia

Primary PSMCs were used to investigate the function of JMJD1C knockdown in vitro. The purity of isolated PSMCs was identified using an α -SMA antibody by immunofluorescence staining (Fig. 5A). To mimic the condition of PSMCs in vivo, PSMCs were exposed to normoxia or hypoxia (1% O_2) for 48 h. The results showed that the expression of JMJD1C was upregulated in PSMCs exposed to hypoxia (Fig. 5B, C). Similar alterations in JMJD1C expression were observed in PSMCs by immunofluorescence staining (Fig. 5D). Then, three pairs of shRNAs targeting JMJD1C were designed to inhibit its expression in vitro (Fig. 5E, F). The hypoxia-induced high expression of JMJD1C in PSMCs was downregulated by the shRNA (Fig. 5G, H). The in vitro results show the potential importance of JMJD1C in PSMCs.

JMJD1C knockdown prevents proliferation and glycolysis in PSMCs exposed to hypoxia

Then, the effect of JMJD1C in vitro was examined. We found that JMJD1C knockdown reduced hypoxia-induced high levels of PASC survival by CCK8 assays (Fig. 6A). The results of Ki67 immunofluorescence staining showed that the hyperproliferation of PSMCs exposed to hypoxia was inhibited by JMJD1C silencing (Fig. 6B). The increases in the protein levels of Cyclin D1 and CDK4 in PSMCs exposed to hypoxia were downregulated by JMJD1C knockdown (Fig. 6C). Similar to the in vivo results, the hypoxia-induced increases in glycolytic enzymes and production of lactate were reduced by JMJD1C inhibition in vitro (Fig. 6D–F). Taken together, the in vitro results suggest that JMJD1C facilitates hyperproliferation and glycolytic processes in hypoxia-induced PSMCs.

STAT3 signaling activation is regulated by JMJD1C and stimulates PASC proliferation and glycolysis

Consistent with the in vivo results, we demonstrated that knockdown of JMJD1C inactivated STAT3 signaling in PSMCs exposed to hypoxia (Fig. 7A). The STAT3 overexpression plasmid was used to explore the underlying mechanism. The results showed that the inhibitory effect of JMJD1C on survival in hypoxia-induced PSMCs was reversed by STAT3 (Fig. 7B). STAT3

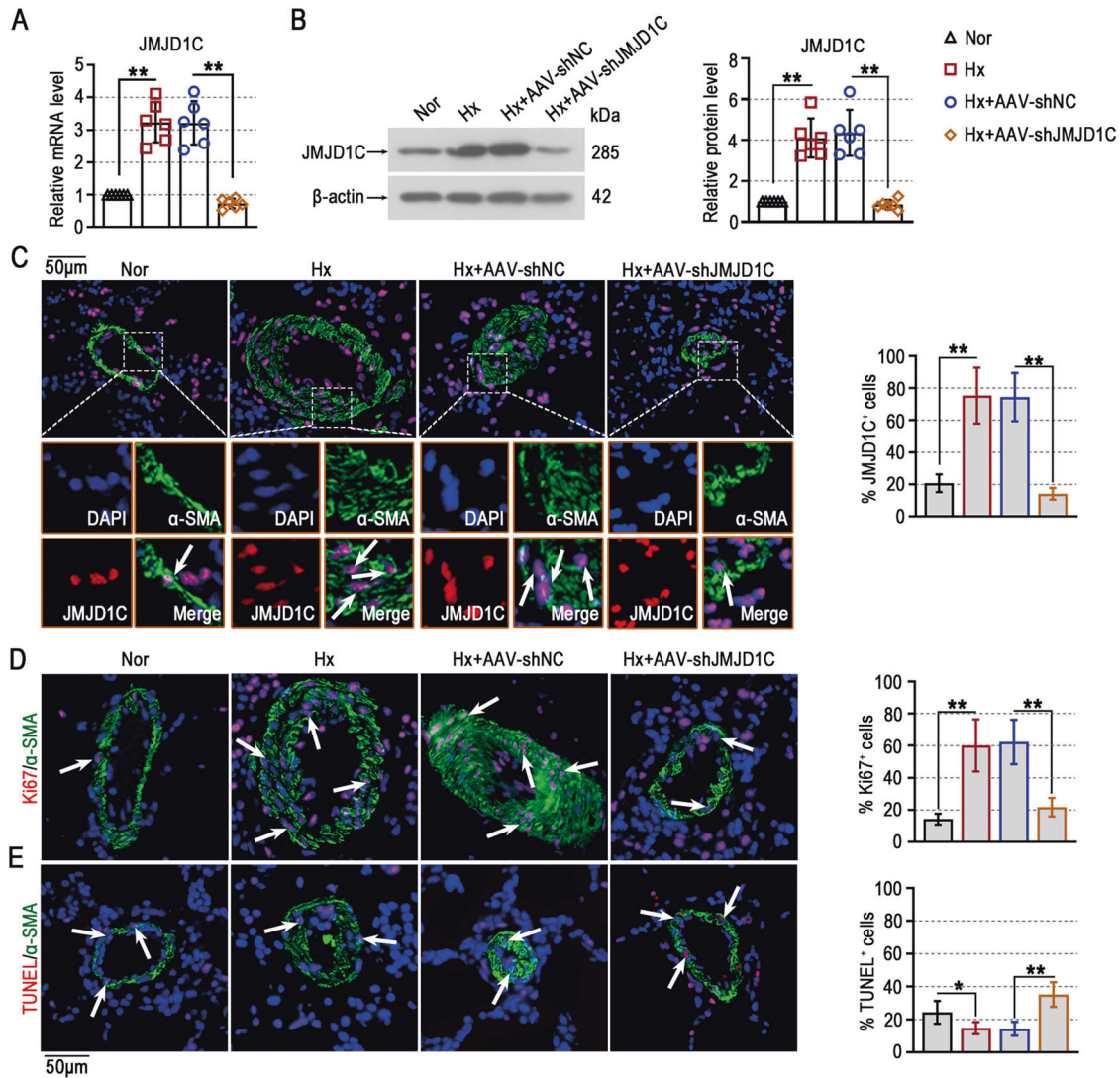


Fig. 3 JMJD1C knockdown decreases PASMC hyperproliferation and resistance to apoptosis in mice exposed to hypoxia. **A, B** The mRNA and protein levels of JMJD1C in lungs were detected using qPCR and Western blotting. **C** Representative lung sections were subjected to immunofluorescence staining of α -SMA (green) and JMJD1C (red) (left panel). DAPI was used to stain cell nuclei (blue). Arrows indicate the coexpression of α -SMA and JMJD1C in pulmonary arteries. The percentage of JMJD1C⁺ cells in pulmonary arteries (stained with α -SMA) was quantified (right panel). Bar = 50 μ m. **D** Representative immunofluorescence images of lung sections stained with anti- α -SMA antibodies (green) and anti-Ki67 antibodies (red) (left panel). DAPI was used to stain cell nuclei (blue). Arrows indicate the colocalization of α -SMA and Ki67 in pulmonary arteries. The percentage of Ki67⁺ cells in pulmonary arteries (stained with α -SMA) was quantified (right panel). Bar = 50 μ m. **E** Representative immunofluorescence images of lung sections stained with anti- α -SMA antibodies (green) and TUNEL (red) (left panel). DAPI was used to stain cell nuclei (blue). Arrows indicate the colocalization of α -SMA and TUNEL in pulmonary arteries. The percentage of TUNEL⁺ cells in pulmonary arteries (stained with α -SMA) was quantified (right panel). Bar = 50 μ m. Nor Normoxia, Hx Hypoxia. The values are the mean \pm SD, and statistical significance was determined by one-way ANOVA. $N = 6$, * $p < 0.05$, ** $p < 0.01$.

overexpression enhanced the reduction in Ki67⁺ cells in JMJD1C-knockdown cells (Fig. 7C). In addition, the JMJD1C knockdown-induced increase in the expression of glycolytic enzymes was reversed by STAT3 (Fig. 7D). Taken together, these results suggest that JMJD1C activates STAT3 signaling to promote hyperproliferation and glycolytic abnormalities in PASMCs exposed to hypoxia.

DISCUSSION

In this study, we demonstrate that high JMJD1C expression promotes pulmonary arterial vascular remodeling and right ventricular hypertrophy in mice exposed to hypoxia. Hypoxia-induced PASMC hyperproliferation and resistance to apoptosis were inhibited by JMJD1C knockdown. The aberrant glycolytic

processes in response to hypoxia mediate the effect of JMJD1C on the development of pulmonary hypertension by activating STAT3 signaling.

It is well documented that a variety of regulatory genes and environmental factors cause the development of PAH, which has complicated pathological mechanisms [17]. Hypoxia is a principal biological phenomenon that exerts significant effects on cell physiology [18], and it has been shown to be correlated with cellular phenotypes, such as proliferation, survival, inflammation and metabolic abnormalities [19–21]. In fact, hypoxia-associated pathways act as critical drivers of various diseases, including cancer, stroke, and PAH [22–24]. Our study showed that significant pathological features associated with PAH in the clinic were observed in mice exposed to hypoxia, as evidenced by pulmonary

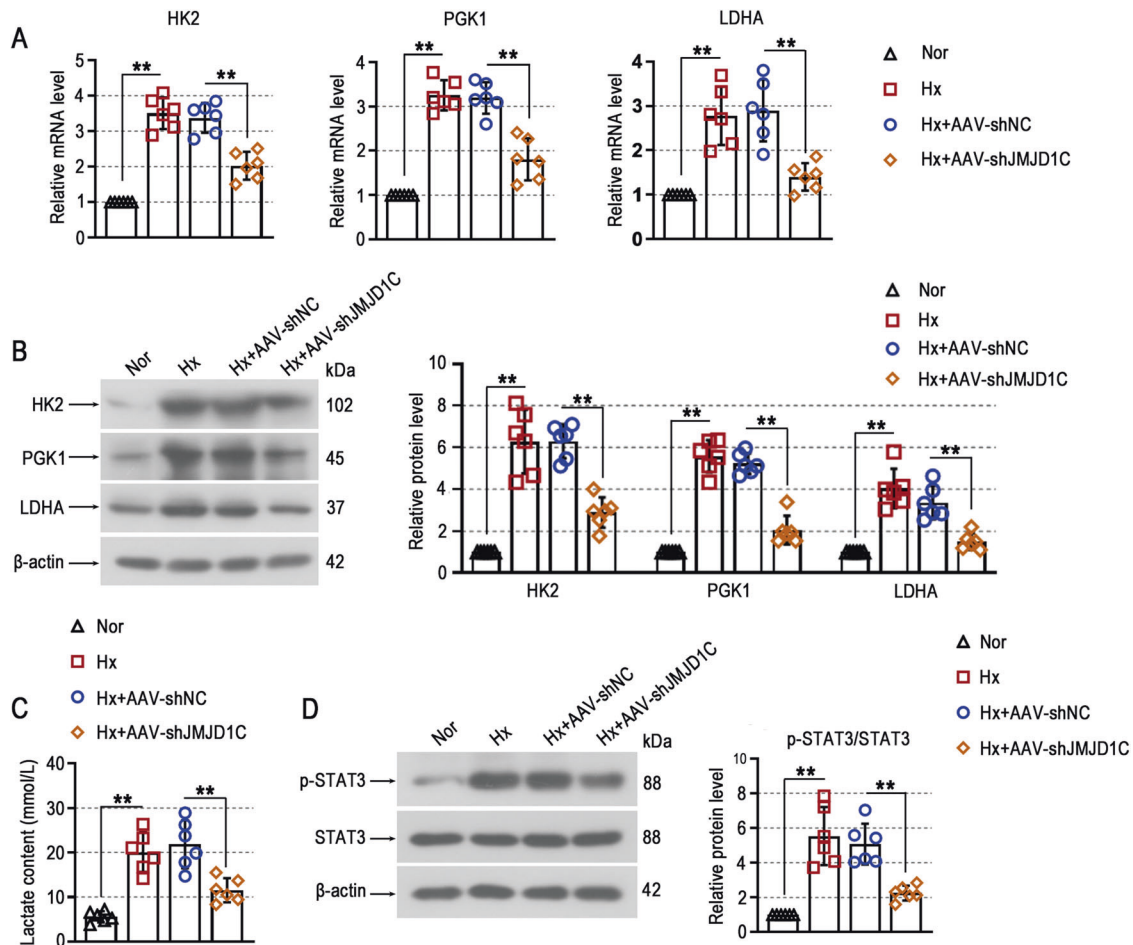


Fig. 4 JMJD1C knockdown prevents glycolysis in mice exposed to hypoxia. **A** The mRNA levels of HK2, PGK1 and LDHA in lung tissues were measured by qPCR. **B** Western blot analysis of HK2, PGK1 and LDHA protein expression in lung tissues. **C** Serum lactate levels were measured. **D** The protein levels of p-STAT3 and STAT3 were examined using Western blotting. Nor Normoxia, Hx Hypoxia. The values are the mean \pm SD, and statistical significance was determined by one-way ANOVA. $N = 6$, ** $p < 0.01$.

vascular remodeling and right ventricular hypertrophy. Previous studies demonstrated that JMJD1C promoted the development of cardiac hypertrophy in angiotensin II-induced mice [13, 14]. In this study, we found that JMJD1C expression was upregulated in mice exposed to hypoxia, and JMJD1C knockdown attenuated the development of pulmonary hypertension.

PASMCs in PAH were reported to become hyperproliferative and resistant to apoptosis, sharing similar features with cancer cells [19]. Liu et al. suggested that inhibiting the proliferation and migration of PASMCs protected against PAH [25]. It has been documented that JMJD1C drives the proliferation, migration, and invasion in a variety of cancers [26–28]. In agreement with these previous studies in cancers, we observed the proliferative and antiapoptotic role of JMJD1C in PASMCs exposed to hypoxia. However, several contradictory studies have shown an antiproliferative effect of JMJD1C on cancer cells. For example, Zhong et al. suggested that JMJD1C blocked cell growth by promoting M1 macrophage polarization in glioma [29]. We thought that the effect of JMJD1C on cell proliferation might be attributed to different pathological states.

Glycolysis is an important metabolic pathway that stimulates ATP production by consuming glucose [30]. Previous studies indicated that a metabolic shift toward glycolysis was observed during the development of PAH [31, 32]. Werle et al. suggested that the regulation of glycolysis controlled the proliferation of vascular smooth muscle cells [33]. In hypoxia-induced pulmonary hypertension, the metabolic shift toward glycolysis was reported

to drive a hyperproliferative phenotype in PASMCs [34]. Kovacs et al. stated that PFKFB3, a key glycolytic regulator, promoted cell proliferation and vascular remodeling by activating glycolytic metabolism in PAH [7]. In this study, the positive regulatory effect of JMJD1C on glycolysis was observed in hypoxia-induced pulmonary hypertension, which was in accordance with that described in acute myeloid leukemia cells [12].

The STAT3 signaling pathway controls pulmonary arterial remodeling in PAH. The inflammatory cytokine IL-6 causes STAT3 activation, which correlates with excessive proliferation and apoptotic resistance in PASMCs [35]. Yerabolu et al. proposed that blocking STAT3-mediated signaling pathways attenuated pulmonary vascular remodeling in experimental PAH models [36]. It was discovered that constitutively active STAT3 was also essential for accelerating glycolysis [37]. Our results showed that STAT3 signaling activation was a potential pathway that mediated the role of JMJD1C in PASMC hyperproliferation and glycolysis. In addition, extracellular matrix (ECM) remodeling and pulmonary arterial wall thickening are the major features of PAH, and they suppress arterial compliance or increase vascular stiffness [38]. The increased production of matrix metalloproteinases could degrade ECM components and promote vascular smooth muscle cell proliferation and migration [39, 40]. IL-6-mediated STAT3 signaling activation was reported to be involved in ECM deposition [41]. Thus, the activation of STAT3 signaling might be induced by IL-6 to regulate ECM remodeling, ultimately contributing to hyperproliferation, apoptosis resistance and glycolysis in PAH.

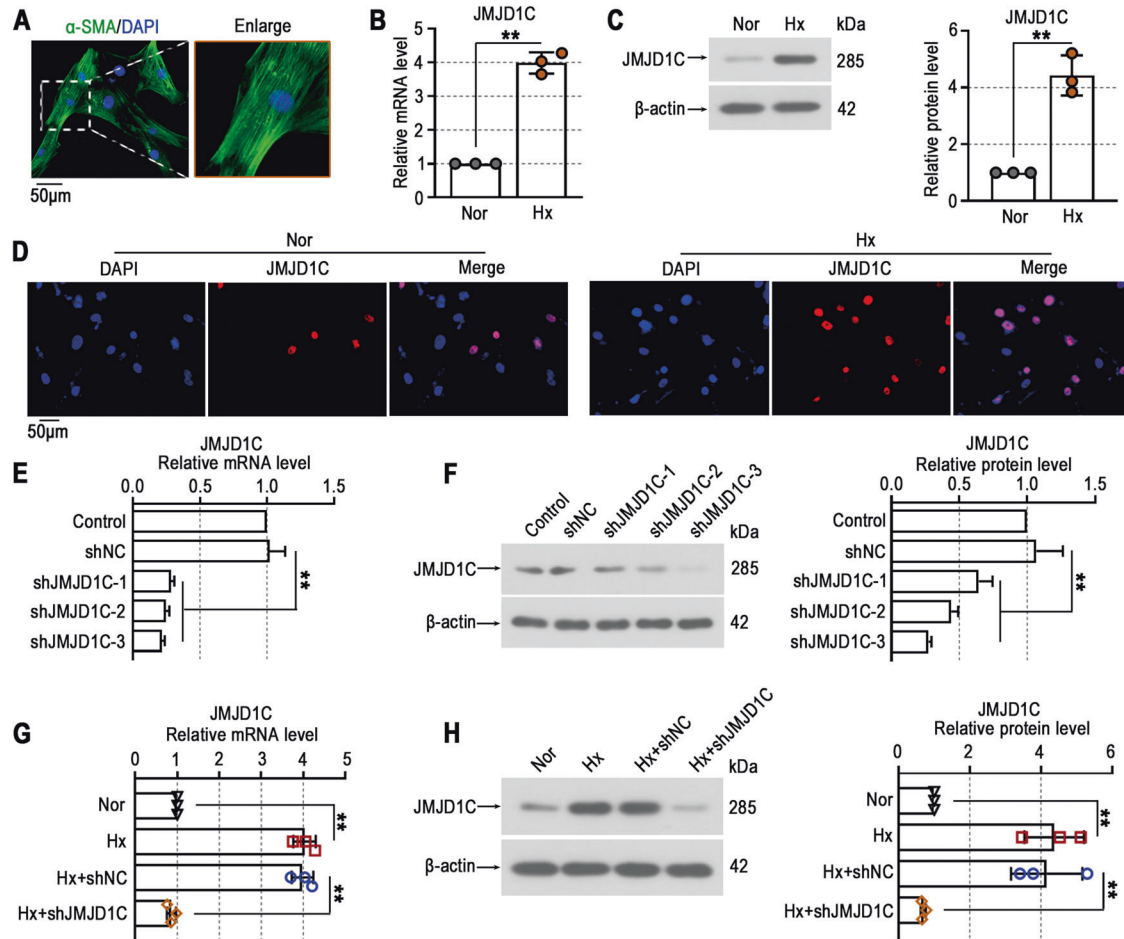


Fig. 5 JMJD1C expression is upregulated in PASCs exposed to hypoxia. **A** Immunofluorescence staining with anti- α -SMA antibodies (green) was performed to determine the purity of PASCs. Cell nuclei were stained with DAPI (blue). Bar = 50 μ m. **B** The mRNA levels of JMJD1C in PASCs were assessed by qPCR. **C** Western blotting was performed to examine JMJD1C protein expression in PASCs. **D** Representative immunofluorescence images of PASCs stained with anti-JMJD1C antibodies (red). Cell nuclei were stained with DAPI (blue). Bar = 50 μ m. **E, G** qPCR analysis of JMJD1C expression in PASCs. **F, H** Western blot analysis of JMJD1C protein levels in PASCs. Nor normoxia, Hx Hypoxia. The values are the mean \pm SD, and statistical significance was determined by unpaired t-test (**B, C**) or one-way ANOVA (**E–H**). $N = 3$, $^{**}p < 0.01$.

In conclusion, the present study shows that high JMJD1C expression contributes to hypoxia-induced vascular remodeling and right ventricular remodeling. The activation of the STAT3 signaling pathway is regulated by JMJD1C and results in a significant proliferative phenotype in PASCs through the enhancement of glycolysis (Fig. 8). This study provides a novel molecular target for developing new therapies for PAH.

MATERIALS AND METHODS

Animal models

Animal protocols were approved by the Ethics Committee of Shengjing Hospital of China Medical University (No. 2019PS106K) and were carried out according to the Guide for the Care and Use of Laboratory Animals. Male C57BL/6 mice (8 weeks; HuaFuKang, Beijing, China) were randomly exposed to normoxia (21% O_2) or hypoxia (10% O_2 and 90% N_2) for 4 weeks as previously described [42]. Briefly, the mice ($n = 72$) were housed in a chamber (ProOx-100HE, TOW-INT TECH, Shanghai, China) with a mixture of oxygen and nitrogen. The oxygen concentration was monitored and controlled by the ProOx-100HE chamber. Soda-lime granules were used to remove CO_2 . All mice were alive and finished the experimental protocols in this study. For the JMJD1C knockdown studies, the synthesized JMJD1C shRNA was cloned into the adeno-associated virus serotype 2 (AAV2) vector. The mice were pretreated with AAV-shJMJD1C or AAV-shNC at a dose of 1.0×10^{10} vg/mouse for one week via tail vein injection.

Analysis of RVSP and RVHI

RVSP and RV hypertrophy were measured to determine the development of pulmonary hypertension. The right cardiac catheterization technique was performed to measure RVSP. In brief, a polyethylene catheter (PE10, Smiths Medical, London, UK) was inserted into the right ventricle through the right jugular vein and connected to a pressure transducer. All data were acquired by a BL420S Biological Signaling Recording and Analysis System (TechMan, Chengdu, China). After the RVSP was measured, the mice were euthanized, and blood, lung and heart were harvested. The RV, left ventricle (LV) and septum (S) were dissected and weighed to calculate the ratio of $RV/(LV + S)$ as an indicator of RVHI.

Histological analysis

To examine the histological changes in pulmonary arteries and RV hypertrophy, fixed lung or heart tissues were embedded in paraffin and sectioned into 5 μ m slices. Then, hematoxylin (H8070, Solarbio, Beijing, China) and eosin (A600190, Sangon, Shanghai, China) were used to stain the sections. Images were captured with an Olympus BX53 microscope (Olympus, Tokyo, Japan) at $\times 200$ or $\times 400$ magnification. To quantify vascular wall thickness, the total vascular area and lumen area were measured blindly, and the ratio of the total vascular area-lumen area to the total vascular area was calculated.

Harvesting mouse PASCs

Primary mouse PASCs were isolated as previously described [42]. Briefly, lung tissues were perfused with PBS, dissected into small pieces and digested

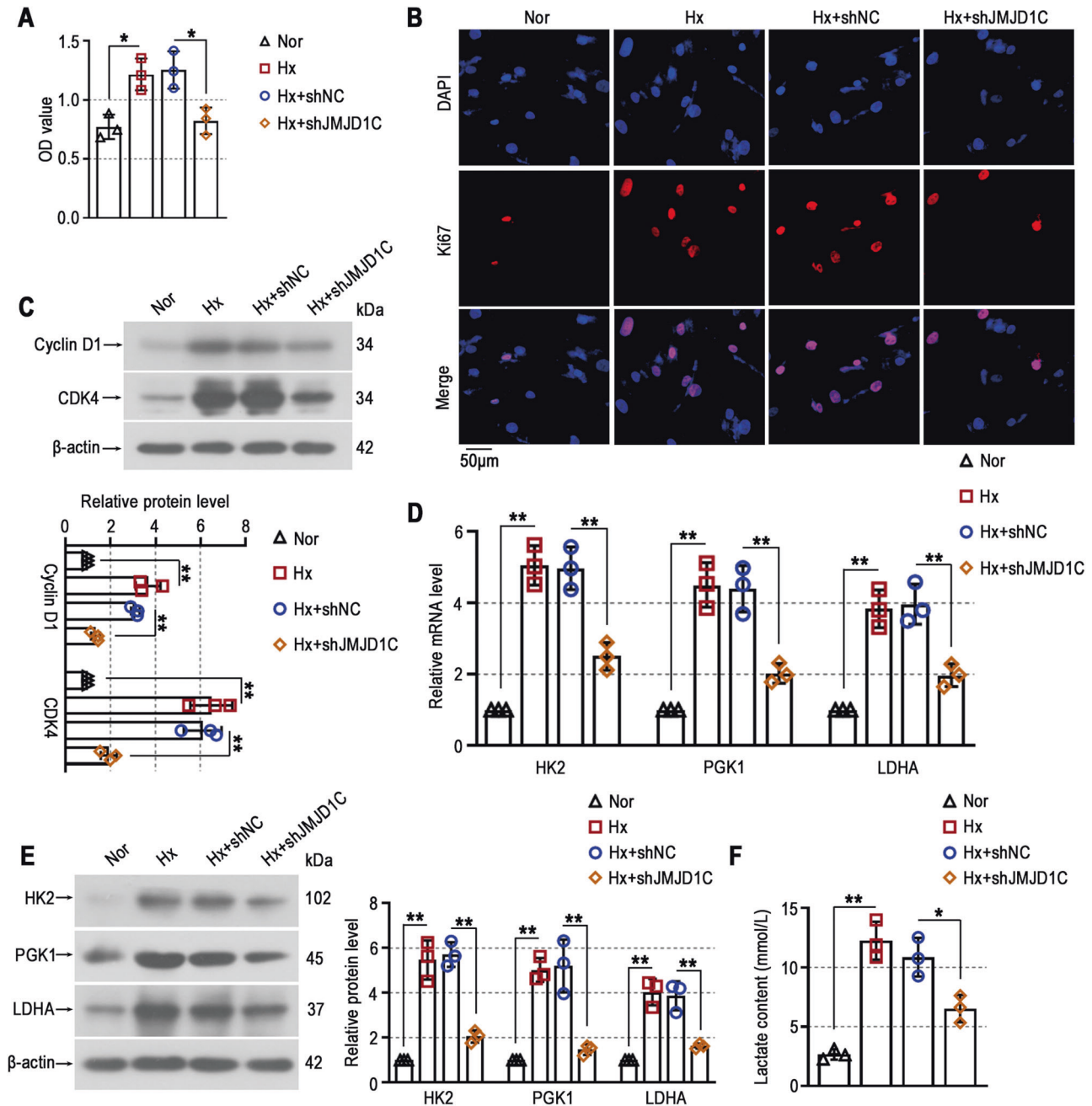


Fig. 6 JMJD1C knockdown prevents proliferation and glycolysis in PASCs exposed to hypoxia. **A** The survival of PASCs was assessed by CCK8 assays. **B** Representative immunofluorescence images of PASCs stained with anti-Ki67 antibodies (red). Cell nuclei were stained with DAPI (blue). Bar = 50 μm. **C** Western blot analysis of Cyclin D1 and CDK4 protein levels in PASCs. **D** The mRNA levels of HK2, PGK1, and LDHA in PASCs were determined by qPCR. **E** Western blot analysis of HK2, PGK1, and LDHA protein levels in PASCs. **F** Cell supernatants were used to assess lactate levels. Nor Normoxia, Hx Hypoxia. The values are the mean ± SD, and statistical significance was determined by one-way ANOVA. $N = 3$, * $p < 0.05$, ** $p < 0.01$.

in PBS containing collagenase type 2 for 30 min at 37 °C. After being centrifuged for 5 min at 4 °C, the resuspended cells were cultured in DMEM (G4510, Servicebio, Wuhan, China) containing 10% FBS in a humidified incubator at 37 °C with 5% CO₂. Immunofluorescent staining was performed to determine the purity of the isolated PASCs by using α-SMA antibodies. Cells at passages 4–7 were prepared for further experiments. Primary PASCs were confirmed to be negative for mycoplasma.

Cell culture and treatment

After being cultured in serum-free medium for 24 h, PASCs were exposed to normoxia (21% O₂) or hypoxia (1% O₂) for 48 h. The constructed plasmid

expressing JMJD1C shRNA (shJMJD1C) or empty vector (shNC) was transfected into PASCs for 24 h to knockdown JMJD1C expression. To examine the function of STAT3 signaling, cells were transfected with a plasmid overexpressing STAT3 (oeSTAT3) for 24 h.

CCK8 assay

To examine cell proliferation, PASCs were seeded in 96-well plates and cultured in DMEM containing 10% FBS. Then, the cells were incubated with CCK8 solution (KGA317, KeyGEN, Nanjing, China) for 2 h, and the OD value was measured using a microplate reader (800Ts, BIOTEK, Winooski, VT, USA) at 450 nm.

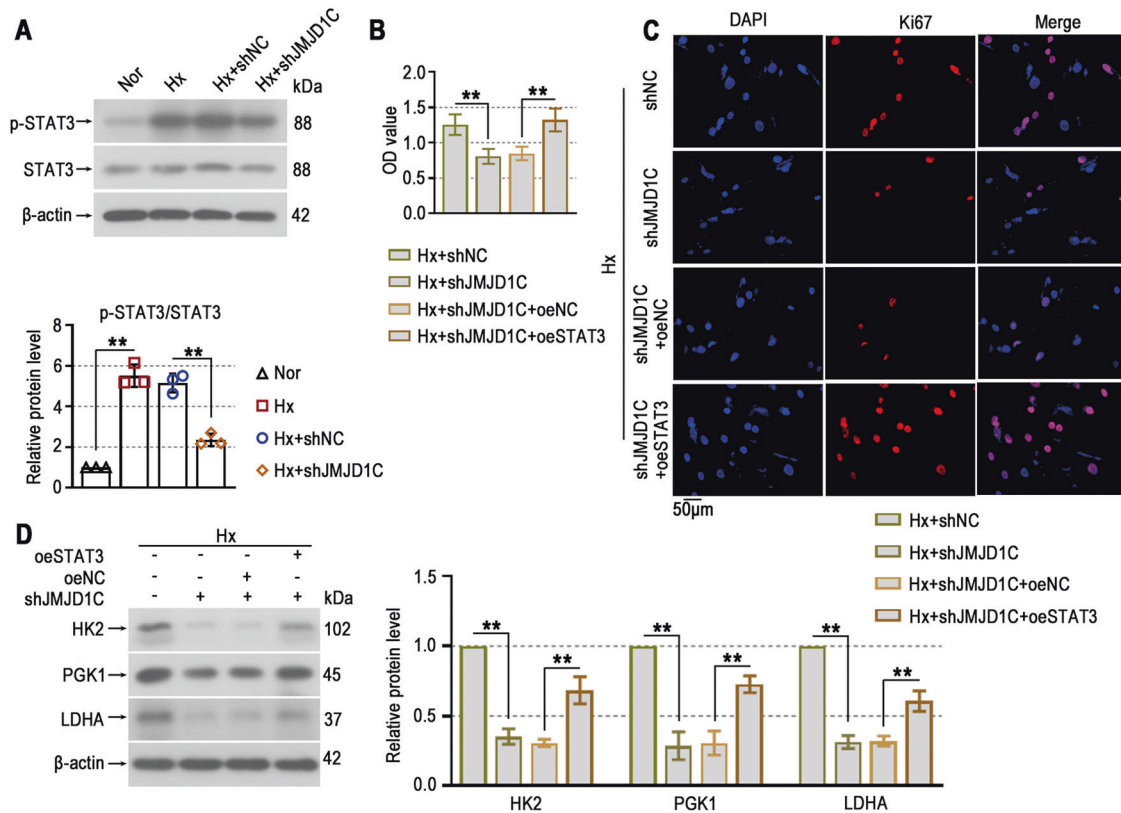


Fig. 7 STAT3 signaling activation is regulated by JMJD1C and stimulates PASM proliferation and glycolysis. **A** Protein levels of p-STAT3 and STAT3 in PASCs were determined by Western blotting. **B** The CCK8 assay was used to examine the survival of PASCs. **C** Representative immunofluorescence images of PASCs stained with anti-Ki67 antibodies (red). Cell nuclei were stained with DAPI (blue). Bar = 50 μm. **D** Western blotting was performed to detect the protein levels of HK2, PGK1, and LDHA in PASCs. Nor Normoxia, Hx Hypoxia. The values are the mean ± SD, and statistical significance was determined by one-way ANOVA. $N = 3$, $**p < 0.01$.

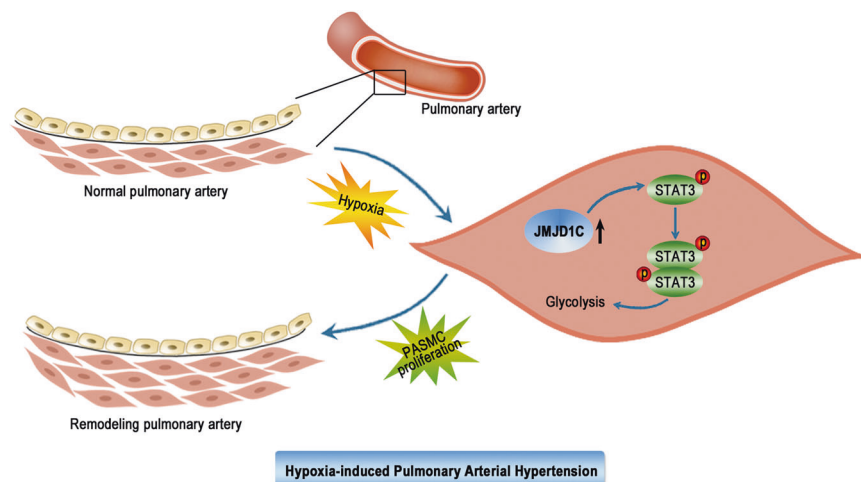


Fig. 8 Schematic illustration of the role of JMJD1C in hypoxia-induced PAH. PASM Pulmonary arterial smooth muscle cell.

Immunofluorescence staining

Double immunofluorescence staining was performed to detect the expression of JMJD1C and Ki67 in pulmonary arteries. The paraffin-embedded slices were incubated with primary antibodies against JMJD1C (1:100; NBP1-77072, Novus Biologicals, Littleton, CO, USA), Ki67 (1:100; AF0198, Affinity, Changzhou, China), or α-SMA (1:200; BF9212, Affinity) overnight at 4 °C. Subsequently, the Cy3-conjugated goat anti-rabbit IgG antibody (1:200; A27039, Invitrogen, Carlsbad, CA, USA) or FITC-conjugated goat anti-mouse IgG antibody (1:200; Ab6785, Abcam, Cambridge, UK) was added and incubated for 90 min at room temperature.

To assess PASM apoptosis in pulmonary arteries, paraffin-embedded sections were stained with an In Situ Cell Death Detection kit (12156792910, Roche, Basel, Switzerland) for 60 min at 37 °C. The α-SMA primary antibody (1:200) was used to stain smooth muscle cells in pulmonary arteries overnight at 4 °C, followed by FITC-conjugated goat anti-mouse IgG antibody (1:200) incubation for 60 min at room temperature.

For in vitro immunofluorescence staining, cells were incubated with primary antibodies against α-SMA (1:100), JMJD1C (1:100) or Ki67 (1:100) overnight at 4 °C, followed by Cy3-conjugated goat anti-rabbit IgG antibody (1:200) or FITC-conjugated goat anti-mouse IgG antibody

(1:200) incubation for 60 min at room temperature. Cell nuclei were counterstained with DAPI. Images were observed under an Olympus microscope at 400× magnification.

Lactate measurement

The lactate levels in serum or cell supernatants were measured by a lactate assay kit (A019, Jiancheng Bio, Nanjing, China) according to the manufacturer's instructions.

Quantitative Real-Time PCR (qPCR)

Total RNA was isolated from lung tissues and PASCs using the TRIpure kit (RP1001, BioTeke, Beijing, China) and reverse-transcribed into cDNA by BeyoRT II M-MLV reverse transcriptase (D7160L, Beyotime, Shanghai, China). The primers for JMJD1C (forward 5'-GTTACCGTCAATATACACG-3', reverse 5'-AACCTTCTCTTATTGG-3'), HK2 (forward 5'-CCCTGCCACCAGACGAAA-3', reverse 5'-CAGCCACAATGTCAATGTCAAAGTC-3'), PGK1 (forward 5'-AGCCAAGATTGTCAAAGA-3', reverse 5'-TTCCCATCAAATACCC-3'), and LDHA (forward 5'-CGGTTCCGTACCTGAT-3', reverse 5'-CTGTCCAACCTGCTT-3') were produced by Genscript (Nanjing, China). qPCR was performed using SYBR Green probes (SY1020, Solarbio) on an Exicycler⁹⁶ Real-Time PCR detection system (Bioneer, Daejeon, Korea). The CT value for each sample was normalized to β -actin, and the relative expression was calculated by the $2^{-\Delta\Delta CT}$ method.

Western blotting

Total protein lysates were extracted with cell lysis buffer (P0013, Beyotime) containing a protease inhibitor (ST506, Beyotime) and quantified with a BCA assay kit (P0011, Beyotime). Protein samples were loaded on SDS-PAGE gels and transferred onto polyvinylidene difluoride membranes. After being blocked in 5% BSA for 1 h at room temperature, the membranes were hybridized with primary antibodies against JMJD1C (1:1000; A20153, ABclonal, Shanghai, China), HK2 (1:1000; A0994, ABclonal), PGK1 (1:1000; A12686, ABclonal), LDHA (1:1000; A0861, ABclonal), p-STAT3 (1:1000; AF3293, Affinity), STAT3 (1:1000; AF6294, Affinity), cyclin D1 (1:1000; A19038, ABclonal), CDK4 (1:1000; A11136, ABclonal) or β -actin (1:1000; sc-47778, Santa Cruz, Dallas, TX, USA) overnight at 4 °C, followed by goat anti-rabbit IgG (1:5000; A0208, Beyotime) or goat anti-mouse IgG (1:5000; A0216, Beyotime) secondary antibody incubation for 45 min at 37 °C. The protein signals were visualized by an enhanced chemiluminescence system (P0018, Beyotime) and quantified using Gel-Pro-Analyzer Software (WD-9413B, Beijing Liuyi Biotechnology Co., Ltd., Beijing, China).

Statistical analysis

All results are expressed as the mean \pm SD. Significant differences was analyzed using GraphPad Prism 8.0 Software (GraphPad Software Inc, La Jolla, CA, USA). Comparisons between two groups were analyzed by unpaired t test, and comparisons among three or more groups were analyzed by one-way ANOVA followed by Bonferroni's multiple comparison test. A *p* value of less than 0.05 indicated significance.

DATA AVAILABILITY

Data that support the findings of this study are available from the corresponding author on reasonable request.

REFERENCES

- Farber HW, Loscalzo J. Pulmonary arterial hypertension. *N Engl J Med*. 2004;351:1655–65.
- Napoli C, Benincasa G, Loscalzo J. Epigenetic inheritance underlying pulmonary arterial hypertension. *Arterioscler, Thromb Vasc Biol*. 2019;39:653–64.
- Culley MK, Chan SY. Mitochondrial metabolism in pulmonary hypertension: beyond mountains there are mountains. *J Clin Invest*. 2018;128:3704–15.
- Zhao L, Ashek A, Wang L, Fang W, Dabral S, Dubois O, et al. Heterogeneity in lung (18)FDG uptake in pulmonary arterial hypertension: potential of dynamic (18)FDG positron emission tomography with kinetic analysis as a bridging biomarker for pulmonary vascular remodeling targeted treatments. *Circulation*. 2013;128:1214–24.
- Bonnet S, Michelakis ED, Porter CJ, Andrade-Navarro MA, Thébaud B, Bonnet S, et al. An abnormal mitochondrial-hypoxia inducible factor-1 α -Kv channel pathway disrupts oxygen sensing and triggers pulmonary arterial hypertension in fawn hooded rats: Similarities to human pulmonary arterial hypertension. *Circulation*. 2006;113:2630–41.

- Calvier L, Boucher P, Herz J, Hansmann G. LRP1 deficiency in vascular smc leads to pulmonary arterial hypertension that is reversed by PPAR γ activation. *Circ Res*. 2019;124:1778–85.
- Kovacs L, Cao Y, Han W, Meadows L, Kovacs-Kasa A, Kondrikov D, et al. PFKFB3 in Smooth Muscle Promotes Vascular Remodeling in Pulmonary Arterial Hypertension. *Am J Respir Crit Care Med*. 2019;200:617–27.
- Kim SM, Kim JY, Choe NW, Cho IH, Kim JR, Kim DW, et al. Regulation of mouse steroidogenesis by WHISTLE and JMJD1C through histone methylation balance. *Nucleic acids Res*. 2010;38:6389–403.
- Wang J, Park JW, Drissi H, Wang X, Xu RH. Epigenetic regulation of miR-302 by JMJD1C inhibits neural differentiation of human embryonic stem cells. *J Biol Chem*. 2014;289:2384–95.
- Viscarra JA, Wang Y, Nguyen HP, Choi YG, Sul HS. Histone demethylase JMJD1C is phosphorylated by mTOR to activate de novo lipogenesis. *Nat Commun*. 2020;11:796.
- Chen M, Zhu N, Liu X, Laurent B, Tang Z, Eng R, et al. JMJD1C is required for the survival of acute myeloid leukemia by functioning as a coactivator for key transcription factors. *Genes Development*. 2015;29:2123–39.
- Lynch JR, Salik B, Connerty P, Vick B, Leung H, Pijning A, et al. JMJD1C-mediated metabolic dysregulation contributes to HOXA9-dependent leukemogenesis. *Leukemia*. 2019;33:1400–10.
- Zhang S, Lu Y, Jiang C. Inhibition of histone demethylase JMJD1C attenuates cardiac hypertrophy and fibrosis induced by angiotensin II. *J Recept Signal Transduct Res*. 2020;40:339–47.
- Yu S, Li Y, Zhao H, Wang Q, Chen P. The Histone Demethylase JMJD1C Regulates CAMKK2-AMPK Signaling to Participate in Cardiac Hypertrophy. *Front Physiol*. 2020;11:539.
- Li Q, Meng L, Liu D. Screening and Identification of Therapeutic Targets for Pulmonary Arterial Hypertension Through Microarray Technology. *Front Genet*. 2020;11:782.
- Edgar R, Domrachev M, Lash AE. Gene Expression Omnibus: NCBI gene expression and hybridization array data repository. *Nucleic Acids Res*. 2002;30:207–10.
- Bull TM, Coldren CD, Geraci MW, Voelkel NF. Gene expression profiling in pulmonary hypertension. *Proc Am Thorac Soc*. 2007;4:117–20.
- Semenza GL. Hypoxia-inducible factors in physiology and medicine. *Cell*. 2012;148:399–408.
- Stenmark KR, Fagan KA, Frid MG. Hypoxia-induced pulmonary vascular remodeling: cellular and molecular mechanisms. *Circ Res*. 2006;99:675–91.
- Maarmar G, Lecour S, Butrous S, Thienemann F, Sliwa K. A comprehensive review: the evolution of animal models in pulmonary hypertension research; are we there yet? *Pulmonary Circ*. 2013;3:739–56.
- Ryan J, Bloch K, Archer SL. Rodent models of pulmonary hypertension: Harmonisation with the world health organisation's categorisation of human PH. *Int J Clin Practice Suppl*. 2011;65:15–34.
- Semenza GL. Oxygen sensing, homeostasis, and disease. *N Engl J Med*. 2011;365:537–47.
- Arumugam TV, Baik SH, Balaganapathy P, Sobey CG, Mattson MP, Jo DG. Notch signaling and neuronal death in stroke. *Prog Neurobiol*. 2018;165–167:103–16.
- Ball MK, Waypa GB, Mungai PT, Nielsen JM, Czech L, Dudley VJ, et al. Regulation of hypoxia-induced pulmonary hypertension by vascular smooth muscle hypoxia-inducible factor-1 α . *Am J Respir Crit Care Med*. 2014;189:314–24.
- Liu H, Wang N, Li J, Wang W, Han W, Li Q. AAV1-Mediated shRNA Knockdown of SASH1 in rat bronchus attenuates hypoxia-induced pulmonary artery remodeling. *Human Gene Ther*. 2021;32:796–805.
- Cai Y, Fu X, Deng Y. Histone demethylase JMJD1C regulates esophageal cancer proliferation Via YAP1 signaling. *Am J Cancer Res*. 2017;7:115–24.
- Chen C, Aihemaiti M, Zhang X, Qu H, Sun QL, He QS, et al. Downregulation of histone demethylase JMJD1C inhibits colorectal cancer metastasis through targeting ATF2. *Am J Cancer Res*. 2018;8:852–65.
- Schimek V, Björn N, Pellé L, Svedberg A, Gréen H. JMJD1C knockdown affects myeloid cell lines proliferation, viability, and gemcitabine/carboplatin-sensitivity. *Pharmacogenet Genom*. 2021;31:60–7.
- Zhong C, Tao B, Yang F, Xia K, Yang X, Chen L, et al. Histone demethylase JMJD1C promotes the polarization of M1 macrophages to prevent glioma by upregulating miR-302a. *Clin Transl Med*. 2021;11:e424.
- Liberti MV, Locasale JW. The Warburg effect: How does it benefit cancer cells? *Trends Biochem Sci*. 2016;41:211–8.
- Paulin R, Michelakis ED. The metabolic theory of pulmonary arterial hypertension. *Circ Res*. 2014;115:148–64.
- Boucherat O, Vitry G, Trinh I, Paulin R, Provencher S, Bonnet S. The cancer theory of pulmonary arterial hypertension. *Pulmonary Circ*. 2017;7:285–99.
- Werle M, Kreuzer J, Höfele J, Elsässer A, Ackermann C, Katus HA, et al. Metabolic control analysis of the Warburg-effect in proliferating vascular smooth muscle cells. *J Biomed Sci*. 2005;12:827–34.

34. Dabral S, Muecke C, Valasarajan C, Schmoranzler M, Wietelmann A, Semenza GL, et al. A RASSF1A-HIF1 α loop drives Warburg effect in cancer and pulmonary hypertension. *Nat Commun.* 2019;10:2130.
35. Paulin R, Meloche J, Bonnet S. STAT3 signaling in pulmonary arterial hypertension. *Jak-stat.* 2012;1:223–33.
36. Yerabolu D, Weiss A, Kojonazarov B, Boehm M, Schlueter BC, Ruppert C, et al. Targeting Jak-Stat signaling in experimental pulmonary hypertension. *Am J Respir Cell Mol Biol.* 2021;64:100–14.
37. Demaria M, Misale S, Giorgi C, Miano V, Camporeale A, Campisi J, et al. STAT3 can serve as a hit in the process of malignant transformation of primary cells. *Cell Death Differ.* 2012;19:1390–7.
38. Thenappan T, Chan SY, Weir EK. Role of extracellular matrix in the pathogenesis of pulmonary arterial hypertension. *Am J Physiol Heart Circ Physiol.* 2018;315:H1322–h31.
39. Chi PL, Cheng CC, Hung CC, Wang MT, Liu HY, Ke MW, et al. MMP-10 from M1 macrophages promotes pulmonary vascular remodeling and pulmonary arterial hypertension. *Int J Biol Sci.* 2022;18:331–48.
40. Hoffmann J, Marsh LM, Pieper M, Stacher E, Ghanim B, Kovacs G, et al. Compartment-specific expression of collagens and their processing enzymes in intrapulmonary arteries of IPAH patients. *Am J Physiol Lung Cell Mol Physiol.* 2015;308:L1002–13.
41. Ghosh A, Pechota A, Coleman D, Upchurch GR Jr, Eliason JL. Cigarette smoke-induced MMP2 and MMP9 secretion from aortic vascular smooth cells is mediated via the Jak/Stat pathway. *Human Pathol.* 2015;46:284–94.
42. Omura J, Satoh K, Kikuchi N, Satoh T, Kurosawa R, Nogi M, et al. ADAMTS8 promotes the development of pulmonary arterial hypertension and right ventricular failure: A possible novel therapeutic target. *Circ. Res.* 2019;125:884–906.

AUTHOR CONTRIBUTIONS

CZ and HYZ performed study concept and design; CZ, YS, YYG, and HYZ performed development of methodology and writing, review and revision of the paper; YS, YYG, and JJX provided acquisition, analysis, and interpretation of data, and statistical analysis. All authors read and approved the final paper.

FUNDING

This study was funded by the Doctoral Startup Foundation of Liaoning Province (No. 2019-BS-288) and the 345 Talent Project of Shengjing Hospital (No. M0735).

COMPETING INTERESTS

The authors declare no competing interests.

ETHICAL APPROVAL

Animal protocols were approved by the Ethics Committee of Shengjing Hospital of China Medical University (No. 2019PS106K) and were carried out according to the Guide for the Care and Use of Laboratory Animals.

ADDITIONAL INFORMATION

Supplementary information The online version contains supplementary material available at <https://doi.org/10.1038/s41420-023-01390-5>.

Correspondence and requests for materials should be addressed to Haiyan Zhao.

Reprints and permission information is available at <http://www.nature.com/reprints>

Publisher's note Springer Nature remains neutral with regard to jurisdictional claims in published maps and institutional affiliations.



Open Access This article is licensed under a Creative Commons Attribution 4.0 International License, which permits use, sharing, adaptation, distribution and reproduction in any medium or format, as long as you give appropriate credit to the original author(s) and the source, provide a link to the Creative Commons license, and indicate if changes were made. The images or other third party material in this article are included in the article's Creative Commons license, unless indicated otherwise in a credit line to the material. If material is not included in the article's Creative Commons license and your intended use is not permitted by statutory regulation or exceeds the permitted use, you will need to obtain permission directly from the copyright holder. To view a copy of this license, visit <http://creativecommons.org/licenses/by/4.0/>.

© The Author(s) 2023